

## Supplementary Information

### Mechanism for spontaneous oxygen and hydrogen evolution on CoO nanocrystals

Kyoung-Won Park<sup>a,b</sup>, Alexie M. Kolpak<sup>c,\*</sup>

<sup>a</sup> Department of Materials Science and Engineering, Massachusetts Institute of Technology, Cambridge, Massachusetts 02139, United States

<sup>b</sup> Center for Biomaterials, Korea Institute of Science and Technology (KIST), Seoul, 02792, Republic of Korea

<sup>c</sup> Department of Mechanical Engineering, Massachusetts Institute of Technology, Cambridge, Massachusetts 02139, United States.

#### Corresponding Author

\* [kolpak@mit.edu](mailto:kolpak@mit.edu)

## 1. $\Delta ZPE - T\Delta S$ of CoO(111) and CoO(100) with adsorbates

**Table S1** Zero point energies (ZPE), entropies and  $\Delta ZPE - T\Delta S$  of CoO(111) and CoO(100) calculated with H, O, OH adsorption at 298K. All vibrational frequencies are calculated under normal mode. The notation of surface configurations is the same as the one in the main manuscript. The unit is eV/adsorbate.

	ZPE	TS	ZPE-TS	$\Delta ZPE - T\Delta S$
H <sub>2</sub> O(l) [1]	0.567	0.670	-0.103	-
H <sub>2</sub> (g) [1]	0.264	0.410	-0.146	-
OH*(1/4)-CoO(111)	0.258	-0.051	0.309	0.3493
OH*(1)-CoO(111)	0.245	-0.050	0.295	0.3345
H*(1/4)-CoO(111)	0.057	-0.012	0.070	0.13
H*(1)-CoO(111)	0.058	-0.013	0.072	0.132
O*(1/4)-CoO(111)	0.022	0.012	0.011	-0.009
O*(1)-CoO(111)	0.023	0.011	0.013	-0.007
H*(1/2)-OH*(1/2)-CoO(111)	0.152	0.038	0.189	0.241
H*(1/4)-CoO(100)	0.113	-0.030	0.143	0.203
H*(1)-CoO(100)	0.112	0.030	0.143	0.203
O*(1/4)-CoO(100)	0.048	-0.008	0.056	0.036
O*(1)-CoO(100)	0.047	0.007	0.054	0.034
OH*(1/4)-CoO(100)	0.222	0.048	0.269	0.309
OH*(1)-CoO(100)	0.211	0.046	0.258	0.298

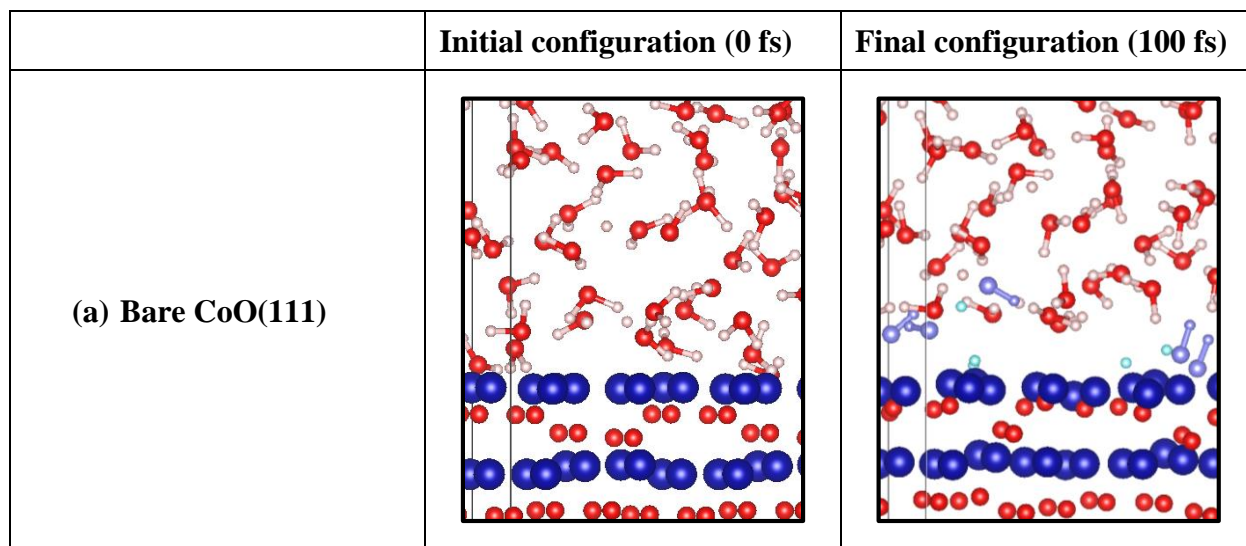
[1] J.Rossmeisl et al., chemical physics 319, 178-184 (2005)

**Table S2.**  $\Delta ZPE - T\Delta S$  used in the calculations of the free energy change throughout the paper. For OOH-adsorbed surface (OOH\*), values of O\* and OH\* are summed.

Surface orientation		$\Delta ZPE - T\Delta S$
<b>CoO(111)</b>	H	0.131
	O	-0.008
	OH	0.342
	OOH	0.334
<b>CoO(100)</b>	H	0.203
	O	0.035
	OH	0.304
	OOH	0.339

## 2. Complexity of CoO(111) surface in an aqueous environment

Figures S1(a) and (b) show atomic configurations of bare CoO(111) and fully hydroxylated CoO(111) (OH\*-CoO(111)) surfaces before and after *ab initio* molecular dynamics (AIMD) relaxation in direct contact with water molecules. The bare CoO(111) surface, which is thermodynamically unstable in an aqueous environment [1], dissociates H<sub>2</sub>O near the surface into -OH and -H and some of the created -OH and -H are adsorbed on the surface. The coverage of OH and H and the atomic configuration of the adsorption are different from the way adsorbates are usually considered on slabs of interest in DFT calculations. On the other hand, the OH\*-CoO(111) surface that is thermodynamically stable in an aqueous environment [1] does not react with water, maintains a surface environment close to the initial state except for thermal vibration due to the elevated temperature effect (at 298 K). This implies that the actual surface environment of CoO(111) formed during the photocatalytic water splitting might be more complex than we have thought, even though the final surface environment becomes closer to the fully hydroxylated CoO(111) after equilibration between CoO(111) and water.



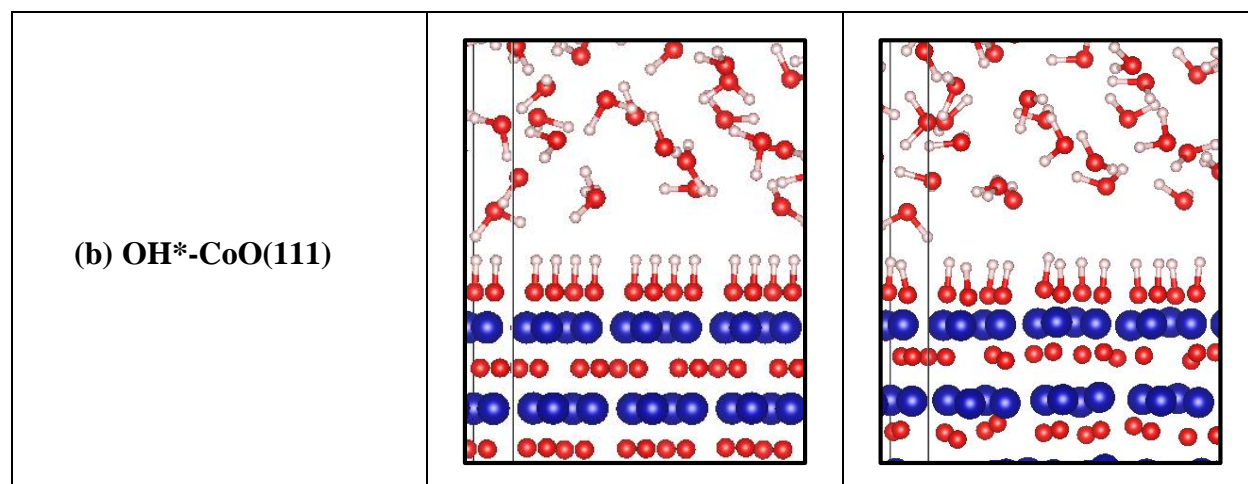


**Fig. S1.** Initial and *ab initio* MD relaxed atomic configurations of (a) bare CoO(111) and (b) OH\*-CoO(111) surfaces in direct contact with water molecules, for 100 fs at 298 K. Blue, red, white circles denote Co, O, H. Light Purple and sky blue indicate OH and H which are formed by dissociation of water on the surface.

[1] K.W. Park, A. M. Kolpak, J. Catal. 365 (2018) 115.

### 3. OER overpotentials vs. CoO(111) surface configurations

We calculate the HER/OER overpotentials for various surface configurations that can be vastly modified during water splitting. Figure S2(a) shows free energy change for intermediate state along reaction coordinates ( $\text{OH}^*$ ,  $\text{O}^*$ ,  $\text{OOH}^*$ ,  $\text{O}_2$ ). Based on the energy diagram, OER overpotentials of the surface configurations at the equilibrium potential (1.23 V) are evaluated as the highest energy change among the intermediates and plotted with respect to OER scaling parameter,  $\Delta G_{\text{O}^*}^0 - \Delta G_{\text{OH}^*}^0$  [1], as shown in Figure S2(b). We find that the OER overpotentials of CoO(111) vary significantly depending on the surface coverage, and the OER overpotentials form a volcano relation with respect to OER scaling parameter ( $\Delta G_{\text{O}^*}^0 - \Delta G_{\text{OH}^*}^0$ ), in good agreement with previous studies of other metal oxide catalysts [1]. Most surface configurations of CoO(111) are on the strong-binding leg of the volcano (left side of the summit), while clean CoO(100) surface is on the weak binding leg in the volcano (right side of the summit) which in turn demonstrates again its poor OER activity. It is also interesting to note that the OER activity of the CoO(111) surface is higher in the more OH covered surface (red shaded region) than in less OH covered surface configuration (green shaded region). Ultimately, the most reactive surface configuration for OER is half hydroxylated CoO(111). This implies that OH adsorption assists OER by reducing the kinetic barrier for the reaction up to critical OH coverage (1/2). The surface configurations of the higher OER overpotentials, i.e.,  $\text{OH}^*(1/2)\text{-CoO}(111)$  and  $\text{OH}^*(3/4)\text{-CoO}(111)$  surfaces, especially have stronger OH binding but weaker O binding unlike the other CoO(111) configurations in Figure S2(a). This tendency is in accordance with the origin of the OER scaling parameter ( $\Delta G_{\text{O}^*}^0 - \Delta G_{\text{OH}^*}^0$ ) showing a lower  $\text{O}_2$ -evolving overpotential is related to a strong OH and weak O bindings to the surface [1].

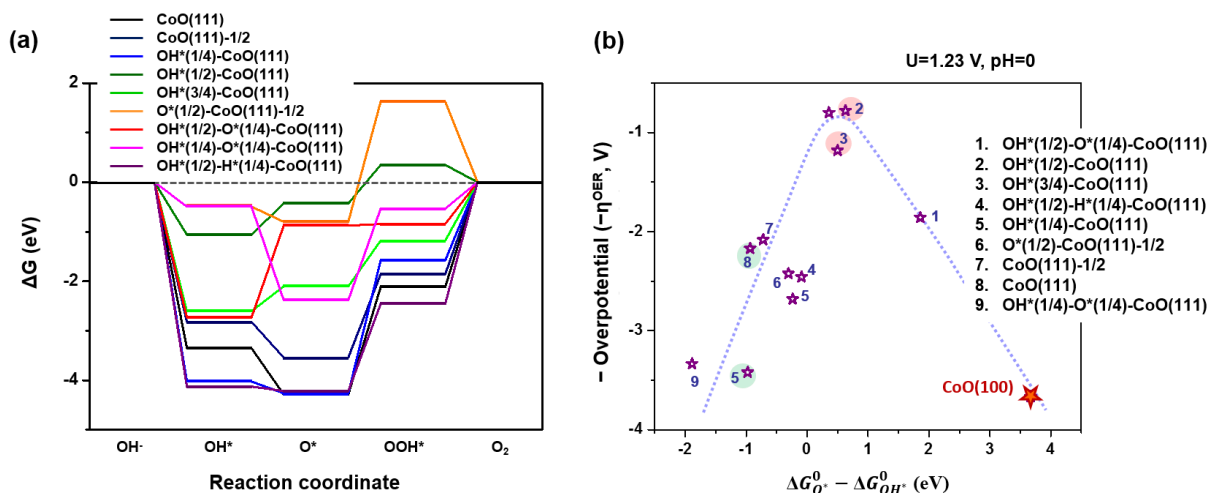
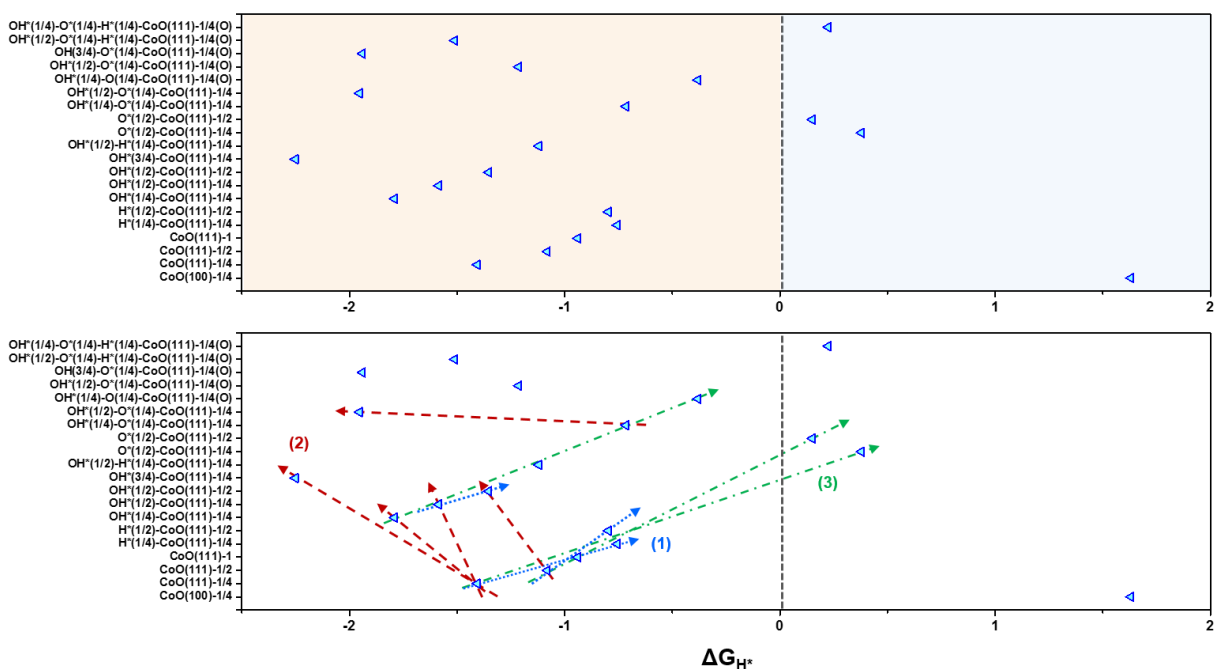


**Fig. S2 (a)** Free energy diagram of CoO(111) surface configurations for oxygen evolution reaction at the equilibrium potential, pH = 0. **(b)** Volcano plot of OER overpotential with respect to OER scaling parameter,  $\Delta G_{O^*}^0 - \Delta G_{OH^*}^0$ , based on the free energy changes in Figure S2(a). OER overpotential of bare CoO(100) surface is marked with a red star in the plot for reference. The notation of surface configurations is the same as the one in the main manuscript.

[1] J. Rossmeisl, Z.-W. Qu, H. Zhu, G.-J. Kroes, J.K. Nørskov, *J. Electroanal. chem.* 607 (2007) 83.

#### 4. $\Delta G_{H^*}$ vs. CoO(111) surface configurations

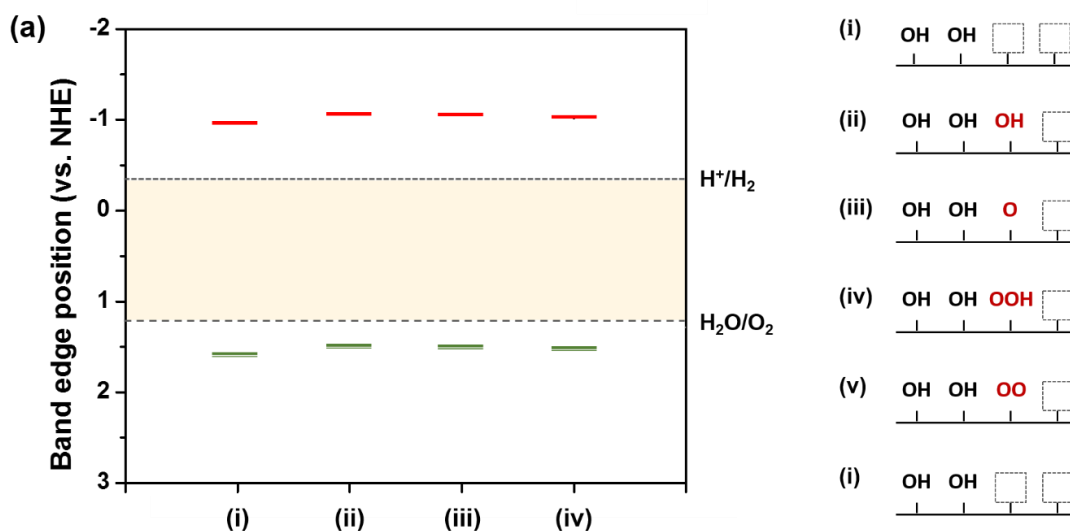
Figure S3 shows free energy change for hydrogen adsorption ( $\Delta G_{H^*}$ ) of CoO(111) with various OH, O and H coverage at standard condition (0 V). As can be seen in Figure S3, the free energy change largely changes depending on the surface configurations from -2.1 – 1.65 eV. Considering that the distance of  $\Delta G_{H^*}$  from 0 directly indicates HER activity, HER activity alters a lot depending on the surface environment. Among the adsorbates (OH, O, H) on the CoO(111), it is found that OH adsorption makes  $\Delta G_{H^*}$  value more negative, and H and O adsorptions have more positive values. Therefore, it is expected that the balanced coverage of the adsorbates can optimize the HER activity of the CoO(111) surface close to 0.



**Fig. S3** Free energy change for hydrogen adsorption ( $\Delta G_{H^*}$ ) of CoO(111) with various OH, O and H coverage at standard condition. The notation of surface configurations is the same as the one in the main manuscript. The bottom figure is shown for the comparison of  $\Delta G_{H^*}$  change when OH, O, and H are adsorbed on the CoO(111) surface. Blue, red, and green dashed lines (denoted with (1), (2), and (3)) point out the OH, H, O adsorption effect.

#### 5. Change of band edge position along the HER/OER pathways

Figures S4(a) and (b) present the change in the conduction/valence band edge position along OER and HER pathways relative to water redox potential at pH=7. The calculation method is explained in ref. [1]. For calculations of the change, the OER is assumed to occur on the OH\*(1/2)-CoO(111) and HER is on bare CoO(100) since these two surface configurations are expected to induce OER and HER under visible light illumination, as explained in terms of incident photon energy vs. reaction kinetic barrier in the main manuscript. Along both reaction pathways, the band edge positions change little. Therefore, the situation such that the potential drop between two facets (CoO(100) and OH\*-CoO(111) in CoO nanoparticles) becomes inverse during the reaction, does not occur. Therefore, the built-in potential in the CoO nanoparticles as well as the charge separation aspect are kept during the overall water splitting reaction, which results in a continuous overall water splitting reaction on the CoO nanoparticles.





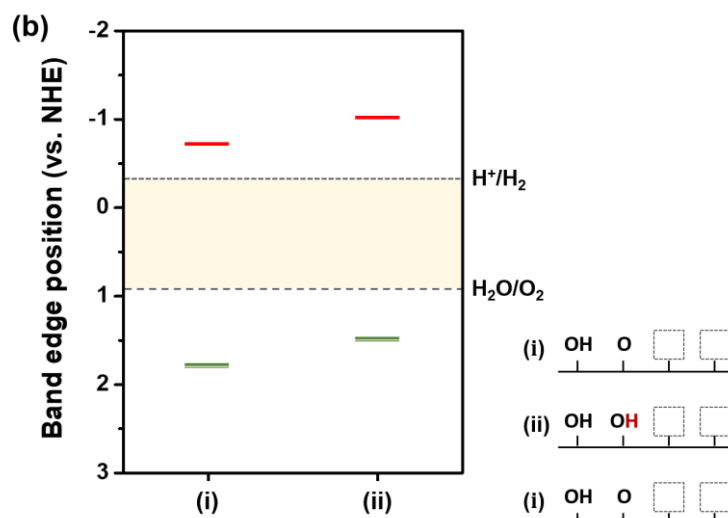


**Fig. S4** Variations of conduction/valence band edge positions (red/green lines) along (a) OER pathways and (b) HER pathways on OH(1/2)\*-CoO(111) at pH=7. The conduction band edge positions relative to water redox potential are calculated with a direct contact of water molecules as explained in ref. [1]. The right side figures of the band edge position show the intermediate states of the OER and HER. The red color characters are adsorbates in each elementary step of the reactions, the dotted line squares are clean surface sites that are uncovered with any adsorbate.

[1] K.W. Park, A. M. Kolpak, J. Cataly. 365 (2018) 115.

## 6. Time required for electron transport in CoO nanoparticles : from OH\*-CoO(111) to CoO(100) facets

Mobility of charge carriers ( $\mu$ ) is defined as  $\mu = \frac{v}{E}$ , where  $v$  = velocity,  $E$  = unit electric field per length.

In CoO nanoparticles with size  $\leq 10$  nm [Ref. 10 in the main text], the built-in potential of 2.19 V is generated due to the potential difference between the CoO(100) and OH\*-CoO(111) facets [Figure 1 in the main text], the CoO nanoparticles will be subjected to the very high unit electric field,  $E \geq 2.19$  V/10 nm.

Velocity of electron ( $v_e$ ) is  $v_e = \mu_e \times E$ .

According to Appendix of a book [1], general II-VI semiconductors have  $\mu_e \cong 0.5$  m<sup>2</sup>/V · s = 500 cm<sup>2</sup>/V · s. Therefore, in CoO nanoparticles with size  $\leq 10$  nm,

$$\begin{aligned} v_e &\geq 500 \frac{\text{cm}^2}{\text{V}\cdot\text{s}} \times \frac{2.19 \text{ V}}{10 \text{ nm}} \\ &\geq 1.095 \times 10^7 \text{ m/s} \end{aligned}$$

Time required for electron transport from OH\*-CoO(111) to CoO(100) facets,

$$t \leq \frac{L}{v} = \frac{10 \text{ nm}}{(1.095 \times 10^7 \text{ m/s})} = \sim 0.9 \text{ fs}$$

[1] Electronic properties of Materials, Rolf E. Hummel, 3<sup>rd</sup> edition